JVI Journals.ASM.org

The nsp1, nsp13, and M Proteins Contribute to the Hepatotropism of Murine Coronavirus JHM.WU

Rong Zhang,[a*] Yize Li,[a] Timothy J. Cowley,[a*] Adam D. Steinbrenner,[a*] Judith M. Phillips,[a] Boyd L. Yount,[b] Ralph S. Baric,[b,c] Susan R. Weiss[a]

Department of Microbiology, Perelman School of Medicine, University of Pennsylvania, Philadelphia, Pennsylvania, USA[a]; Departments of Epidemiology[b] and Microbiology and Immunology,[c] University of North Carolina at Chapel Hill, Chapel Hill, North Carolina, USA

ABSTRACT

Mouse hepatitis virus (MHV) isolates JHM.WU and JHM.SD promote severe central nervous system disease. However, while JHM.WU replicates robustly and induces hepatitis, JHM.SD fails to replicate or induce pathology in the liver. These two JHM variants encode homologous proteins with few polymorphisms, and little is known about which viral proteins(s) is responsible for the liver tropism of JHM.WU. We constructed reverse genetic systems for JHM.SD and JHM.WU and, utilizing these full-length cDNA clones, constructed chimeric viruses and mapped the virulence factors involved in liver tropism. Exchanging the spike proteins of the two viruses neither increased replication of JHM.SD in the liver nor attenuated JHM.WU. By further mapping, we found that polymorphisms in JHM.WU structural protein M and nonstructural replicase proteins nsp1 and nsp13 are essential for liver pathogenesis. M protein and nsp13, the helicase, of JHM.WU are required for efficient replication *in vitro* and in the liver *in vivo*. The JHM.SD nsp1 protein contains a K194R substitution of Lys194, a residue conserved among all other MHV strains. The K194R polymorphism has no effect on *in vitro* replication but influences hepatotropism, and introduction of R194K into JHM.SD promotes replication in the liver. Conversely, a K194R substitution in nsp1 of JHM.WU or A59, another hepatotropic strain, significantly attenuates replication of each strain in the liver and increases IFN-β expression in macrophages in culture. Our data indicate that both structural and nonstructural proteins contribute to MHV liver pathogenesis and support previous reports that nsp1 is a *Betacoronavirus* virulence factor.

IMPORTANCE

The *Betacoronavirus* genus includes human pathogens, some of which cause severe respiratory disease. The spread of severe acute respiratory syndrome coronavirus (SARS-CoV) and Middle East respiratory syndrome coronavirus (MERS-CoV) into human populations demonstrates the zoonotic potential of emerging coronaviruses, and there are currently no vaccines or effective antivirals for human coronaviruses. Thus, it is important to understand the virus-host interaction that regulates coronavirus pathogenesis. Murine coronavirus infection of mice provides a useful model for the study of coronavirus-host interactions, including the determinants of tropism and virulence. We found that very small changes in coronavirus proteins can profoundly affect tropism and virulence. Furthermore, the hepatotropism of MHV-JHM depends not on the spike protein and viral entry but rather on a combination of the structural protein M and nonstructural replicase-associated proteins nsp1 and nsp13, which are conserved among betacoronaviruses. Understanding virulence determinants will aid in the design of vaccines and antiviral strategies.

Mouse hepatitis virus (MHV) is an enveloped, nonsegmented, positive-strand RNA virus that belongs to the order *Nidovirales*, family *Coronaviridae*, and genus *Betacoronavirus* (1). Betacoronaviruses can have significant effects on human (2) and animal (3) health. Most notably, the emergent pathogens severe acute respiratory syndrome coronavirus (SARS-CoV) and Middle East respiratory syndrome coronavirus (MERS-CoV) cause severe respiratory disease with significant mortality (4). Thus, it is important to understand the coronavirus-encoded determinants of tropism and virulence. MHV is a model coronavirus that infects the livers and brains of laboratory mice, causing acute hepatitis, encephalitis, and chronic demyelinating disease in an MHV strain-specific manner (5). We use MHV infection of the mouse to study the virus and host determinants of pathogenesis during infection of the liver and central nervous system (CNS).

Previous studies demonstrated that both viral spike protein-mediated entry and non-spike-associated postentry events significantly influence MHV tropism. For example, a single Q159L substitution within the amino-terminal receptor-binding domain of the S1 subunit of the spike protein of the dualtropic A59 strain was sufficient to abrogate hepatotropism but had little effect on CNS

Received 8 December 2014 Accepted 7 January 2015

Accepted manuscript posted online 14 January 2015

Citation Zhang R, Li Y, Cowley TJ, Steinbrenner A, Phillips JM, Yount BL, Baric RS, Weiss SR. 2015. The nsp1, nsp13, and M proteins contribute to the hepatotropism of murine coronavirus JHM.WU. J Virol 89:3598–3609. doi:10.1128/JVI.03535-14.

Editor: S. Perlman

Address correspondence to Susan R. Weiss, weisssr@upenn.edu.

* Present address: Rong Zhang, Division of Infectious Diseases, School of Medicine, Washington University in St. Louis, St. Louis, Missouri, USA; Timothy J. Cowley, 13711 N.E. 10th Pl., Apt. 102, Bellevue, Washington, USA; Adam Steinbrenner, Department of Plant and Microbial Biology, University of California, Berkeley, Berkeley, California, USA.

R.Z. and Y.L. contributed equally to this article.

doi:10.1128/JVI.03535-14

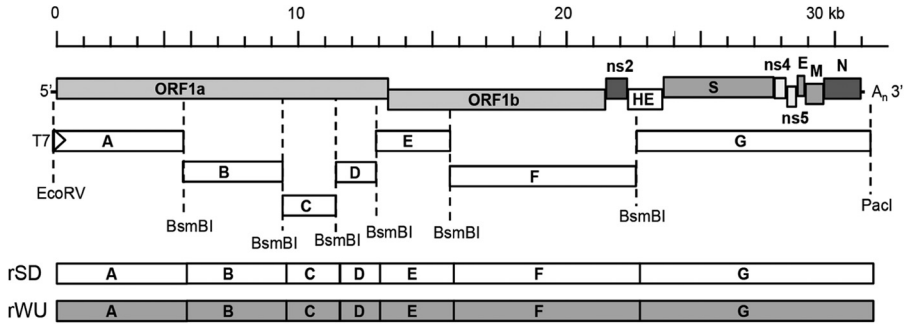

FIG 1 MHV genome organization and the full-length JHM.WU and JHM.SD cDNA clones. The full-length viral genomes were amplified as fragments A to G, which were cloned individually into plasmids. BsmBI type II restriction sites were added to the internal termini of each of the fragments and used for assembly. A T7 promoter for *in vitro* RNA transcription was added to the 5′ end of fragment A. The full-length genomic cDNAs were assembled *in vitro* and the viruses recovered from each designated rSD for JHM.SD and rWU for JHM.WU.

pathogenesis, and hepatotropic revertants had compensatory mutations in the heptad repeat domain of the S2 subunit (6). A long hypervariable domain within the amino-terminal spike subunit S1 has been associated with the ability to spread independently of the viral receptor CEACAM1a and with the high neurovirulence of the JHM.SD strain (7). Substitutions within the heptad repeat domains of the spike have caused defects in spike-induced cell-to-cell fusion and limited spread in the brain (8, 9). In addition, the replicase and other nonstructural proteins have also been identified as liver virulence factors. A mutation within the ADP-ribose-1″-phosphatase (ADRP), the macrodomain of the nsp3 protein, that abolished enzymatic activity attenuated hepatitis compared to wild-type (wt) virus but did not significantly reduce replication in the liver (10), and it recently was found to reduce replication and pathogenesis in the CNS (11). Accessory protein ns2 is a 2′,5′-phosphodiesterase (PDE) that cleaves 2′,5′-oligoadenylates, thereby blocking the activation of RNase L. Mutation of ns2 abolishes PDE activity and attenuates viral replication in the liver and the consequent hepatitis without substantially affecting CNS infection (12).

The JHM.SD isolate of MHV is highly neurovirulent but fails to replicate in the liver and cause hepatitis even when inoculated at doses as high as 10^5 PFU (13); in contrast, the dualtropic (highly neurotropic/highly hepatotropic) JHM.WU replicates to very high titer in the liver (14). JHM.SD encodes wild-type nsp3-ADRP and ns2-PDE but still does not cause hepatitis, suggesting that additional proteins mediate liver pathogenicity. In order to identify such virulence determinants, we used a reverse genetic approach and constructed full-length cDNA clones representing JHM.WU (14, 15) and JHM.SD (16). By exchanging fragments of the genomes and constructing site-directed mutants, we identified the nsp1, nsp13, and M proteins as contributors to JHM replication in the liver.

MATERIALS AND METHODS

Cell lines, mice, and viruses. Recombinant JHM.SD (RJHM/A) (13, 16), which was based on the MHV-4 isolate of JHM (16) and previously recovered by RNA-targeted recombination, and JHM.WU (previously called wb-3) (14, 15) were used as templates to generate infectious cDNA clones. Mildly neurotropic and moderately hepatotropic recombinant rA59 was derived from an existing infectious cDNA clone (17, 18). The mouse 17Cl-1 and L2 fibroblast cell lines and baby hamster kidney cells constitutively expressing MHV receptor CEACAM-1 (BHK-MHVR) were cultured as described previously (17, 19). Primary bone marrow-derived macrophages (BMM) were generated from the hind limbs of B6 or type I interferon receptor-deficient ($IFNAR^{-/-}$) mice as described previously and cultured in Dulbecco modified Eagle medium (DMEM) supplemented with 10% fetal bovine serum (FBS), 1 mM pyruvate, and 30% L929 cell-conditioned medium for 6 days before infection (20). BMM cultures were routinely ≥99% pure as assessed by positive staining for expression of CD11b and negative staining for expression of CD11c. C57BL/6 (B6) mice were purchased from the National Cancer Institute (Frederick, MD) and bred in the University of Pennsylvania animal facility according to procedures approved by the University IACUC.

Construction of JHM.SD and JHM.WU infectious cDNA clones. The strategy employed to construct the infectious cDNA clone of JHM.SD was as described previously for A59 (17) with slight modification. Intracellular RNA was extracted from recombinant JHM.SD (RJHM/A)-infected 17Cl-1 cells and reverse transcribed using SuperScript II (Invitrogen, Carlsbad, CA) and random hexamer primers. The cDNA was amplified by PCR with Expand Long TAQ polymerase (Roche, Mannheim, Germany) to create six fragments (A to F) (Fig. 1). Fragment A was cloned into pCR4 TOPO TA (Invitrogen) and fragments B through F into pSMART-LCAmp (Lucigen). Fragment G was derived from viral sequences in pJHM (21), which were modified to add a BsmBI site at the 5′ end. All of the BsmBI restriction sites encoded within the genome were removed by PCR-based site-directed mutagenesis. BsmB1 restriction sites flanking each of the fragments, as well as the EcoRV site at the 5′ end of fragment A and the PacI site at the 3′ end of fragment G, were introduced during the construction and were used for full-length *in vitro* genome assembly (Fig. 1).

The infectious JHM.WU cDNA clone was constructed using the JHM.SD fragments as a scaffold. Fragments A, C, F, and G were PCR amplified from intracellular RNA extracted from JHM.WU (wb-3)-infected 17Cl-1 cells (15) and inserted into the JHM.SD plasmids in place of the corresponding fragments. The endogenous BsmBI sites were removed as for JHM.SD (Fig. 1). JHM.SD fragments B, D, and E were used for JHM.WU because the proteins encoded by these fragments have complete amino acid sequence identity between the two isolates. All of the primers used for plasmid construction and mutation are available upon request. All of the chimeric and mutant clones used for virus recovery were verified by nucleotide sequencing. A schematic diagram of the construction of the rJHM.SD and rJHM.WU full-length clones is shown in Fig. 1.

Recovery of recombinant viruses. The full-length genomic cDNAs were assembled and the recombinant viruses were recovered as previously described (17, 18). Briefly, JHM.SD and JHM.WU plasmids A through G were digested with BsmBI and isolated from agarose gels. Equal molar ratios of each fragment were ligated (about 2 μg of DNA total) with T4 DNA ligase overnight at 16°C. The ligated DNA was chloroform extracted and precipitated. *In vitro* transcription driven by a T7 promoter present directly upstream of the viral DNA was carried out using the mMessage

mMachine T7 transcription kit (Ambion) (17). The nucleocapsid gene was amplified from each G plasmid with primers bearing the SP6 promoter and then similarly transcribed with the mMessage mMachine SP6 transcription kit. The viral genome transcripts were combined with the N gene transcripts and electroporated into the BHK-MHVR with three pulses of 850 V at 25 μF using a Gene Pulser II electroporator (Bio-Rad, Hercules, CA), and these cells were overlaid on nearly confluent L2 cells. When viral cytopathology was observed, the combined cells and supernatant were harvested. Recombinant viruses were plaque purified and amplified in 17Cl-1 cells. Recombinant JHM.SD will be referred to as rSD and JHM.WU as rWU here.

Generation of chimeric and mutant recombinant viruses. To generate the chimeric JHM.SD expressing the spike gene of WU (rSD.S_{WU}), the portion of the spike gene containing the JHM.WU polymorphism was amplified from the JHM.WU G fragment and cloned into the AvrII and SphI sites of the JHM.SD G fragment (see Fig. 3A). The chimeric JHM.WU with the entire JHM.SD spike gene (rWU.S_{SD}) was constructed by replacing the BamHI-SphI fragment containing the spike gene. The chimeric JHM.SD viruses containing the F and/or G fragment of JHM.WU were constructed by combining JHM.SD fragments A through E with the F and/or G fragment from JHM.WU. The resulting viruses were designated rSD.F_{WU}, rSD.G_{WU}, and rSD.$F_{WU}G_{WU}$. Similarly, rWU.A_{SD} and rWU.C_{SD} were generated by replacing the A and C fragments, respectively, of JHM.WU with those of JHM.SD. Single mutations were constructed by PCR-based site-directed mutagenesis and verified by nucleotide sequencing.

Viral replication kinetics. L2 or BMM cells were infected with each virus at a multiplicity of infection (MOI) of 0.01 or 1 PFU/cell, as indicated. After 1 h, the cells were washed and cultured with DMEM supplemented with 10% FBS. The culture supernatants were collected at the indicated time points, and the virus titers were determined by plaque assays on L2 cells (22).

ELISA. IFN-β protein in the supernatant of MHV-infected BMM was quantified using a commercial capture enzyme-linked immunosorbent assay (ELISA) kit (PBL Laboratories, Piscataway, NJ) according to the manufacturer's instructions.

Mouse infections. Viruses were diluted into phosphate-buffered saline (PBS) containing 0.75% bovine serum albumin. Four-week-old B6 mice were anesthetized with isoflurane (IsoFlo; Abbott Laboratories) and inoculated intrahepatically (i.h.) or intracranially (i.c.) with each virus at the indicated dose. On day 5 postinfection (p.i.), the mice were sacrificed and perfused with PBS. The livers and/or brains were harvested and homogenized and their virus titers determined by plaque assays on L2 cells as previously described (23). All mouse procedures were reviewed and approved by the University of Pennsylvania IACUC.

Histology. The livers were isolated and fixed in 4% paraformaldehyde, embedded in paraffin, and sectioned. Liver sections were stained with hematoxylin and eosin.

Statistical analysis. A two-tailed Student *t* test was performed to assess statistical significance for *in vitro* experiments. The Mann-Whitney test was used to analyze differences in virus titer in mouse tissues. Any undetectable titer from *in vitro* or *in vivo* infection was entered as the limit of detection for the corresponding experiment. All data were analyzed using GraphPad Prism software (GraphPad Software, Inc., CA).

RESULTS

Construction of JHM.SD and JHM.WU reverse genetic systems and comparison of recombinant and parental wild-type viruses. The construction of the full-length cDNA clones for JHM.SD and JHM.WU (1) is described in detail in Materials and Methods and summarized briefly here. Using the genomic RNA of wt recombinant JHM.SD (RJHM/A) previously generated by targeted recombination (24) as a template, seven DNA fragments (A to G) spanning the entire genome were amplified and cloned into bacterial plasmids. A T7 promoter was introduced at the 5′ end of the A fragment (Fig. 1). Cleavage sites for the type II restriction enzyme BsmBI were introduced at the junction sites of each fragment, and all endogenous BsmBI sites were removed by introduction of noncoding mutations (Fig. 1). Other than the nine silent mutations used to remove the BsmBI sites within the genome, the cloned fragments are identical to the sequence of JHM.SD (RJHM/A; GenBank: FJ647219.1). The seven fragments were digested from vectors and assembled into a full-length genomic cDNA. Viral RNA was transcribed using the 5′ T7 promoter and electroporated into BHK-MHVR cells to generate the recombinant JHM.SD, which will be referred to herein as rSD.

For construction of the JHM.WU infectious clone, fragments A, C, F, and G were amplified from JHM.WU (wb-3) genomic RNA and cloned into bacterial vectors as described above. Because there were no amino acid difference in the proteins encoded within the B, D, and E fragments of JHM.WU and JHM.SD, the JHM.SD fragments were used to complete the full genomic cDNA of JHM.WU (Fig. 1). Other than the nine silent mutations used to remove the BsmBI sites, and three synonymous point substitutions in nsp1 and nsp3, the cloned fragments are identical to the sequence of JHM.WU (JHM.WU; GenBank: JX169867.1). Recombinant JHM.WU (referred to as rWU) was recovered as for rSD.

To compare the phenotypes of rSD and rWU with those of their parental viruses, we first determined their replication kinetics (at a low MOI, 0.01 PFU/cell) in murine L2 fibroblasts. Neither the kinetics of replication nor the final titer differed between JHM.SD and its infectious-clone counterpart rSD or between JHM.WU and rWU (Fig. 2A). Of note, JHM.WU and rWU replicated faster than JHM.SD and rSD and to a peak titer 100- to 1,000-fold higher at 36 h postinfection.

Next, we compared replication of rWU and rSD with that of their respective parental viruses *in vivo* in mice. Previous studies demonstrated that intracranial (i.c.) inoculation of weanling C57BL/6 (B6) mice with JHM.SD or JHM.WU caused severe encephalitis (13, 15, 16, 25) but that only JHM.WU caused hepatitis (13, 14). Following i.c. infection of B6 mice, the titer of rSD was approximately 4.7×10^6 PFU g^{-1} of brain, similar to that of wild-type JHM.SD, while rWU, like JHM.WU, replicated to an approximately 10-fold-higher titer (Fig. 2B). In both JHM.SD-infected and rSD-infected mice, the viral titers in the liver were below the limit of detection by plaque assay (about 100 PFU g^{-1}); in contrast, approximately 10^6 PFU g^{-1} of virus was detected in the livers of JHM.WU-infected and rWU-infected mice (Fig. 2B). Following intrahepatic (i.h.) inoculation, JHM.WU and rWU replicated in the liver to an even higher titer, approximately 10^7 PFU g^{-1}, whereas replication of JHM.SD and rSD was below the level of detection (Fig. 2C), as previously observed (24). Previous studies in our lab had indicated that the extent of hepatitis (inflammation and necrosis) in MHV-infected mice correlates with the extent of infectious virus replication in the liver (24). Indeed, hematoxylin and eosin staining demonstrated severe liver necrosis in rWU-infected mouse liver, while no obvious liver damage was observed in rSD-infected mice (Fig. 2D). These results indicated that rSD and rWU reproduced the pathogenesis of their parental isolates JHM.SD and JHM.WU in the mouse model.

Exchange of the JHM.WU and JHM.SD spike proteins does not affect replication in the liver. Relative to the JHM.SD spike, the JHM.WU spike has a 141-amino-acid in-frame deletion (JHM.SD residues 454 to 594) within the S1 subunit hypervariable

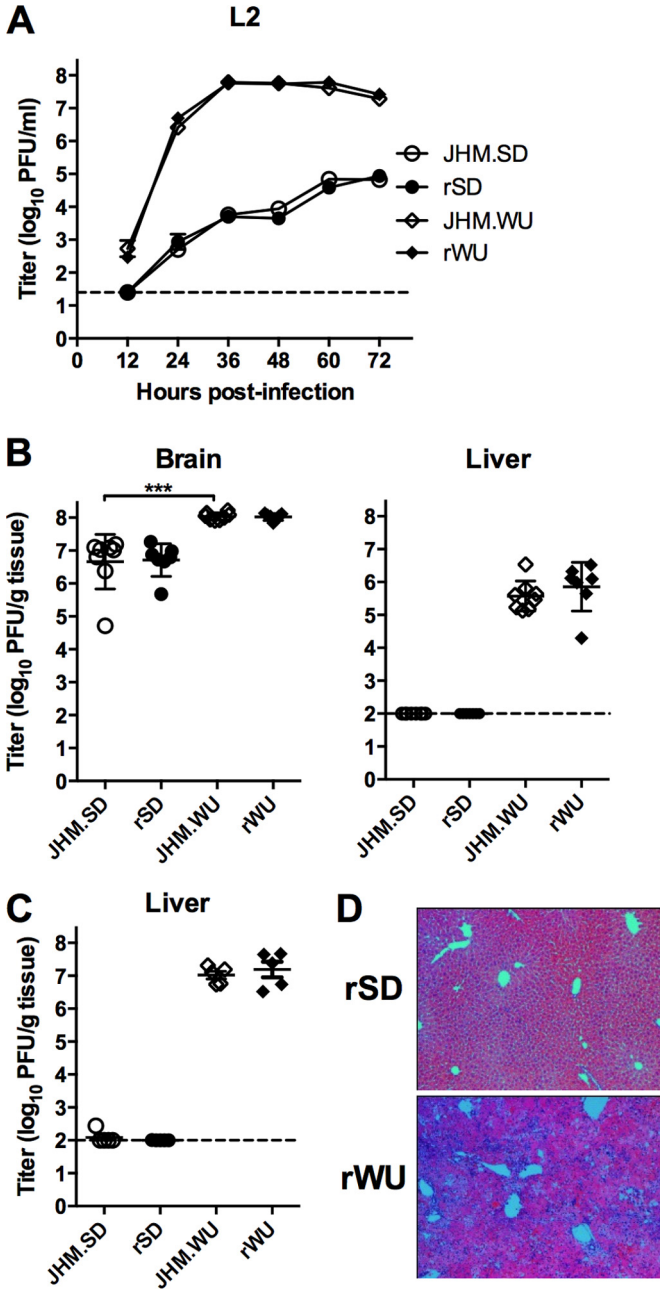

FIG 2 Comparison of recombinant and parental wild-type JHM.SD and JHM.WU *in vitro* and *in vivo*. (A) L2 cells were infected (in triplicate) with JHM.SD, rSD, JHM.WU, and rWU (MOI = 0.01 PFU/cell), and supernatants were collected at the indicated times and the virus titers determined. (B) Mice ($n = 7$ or 8) were infected i.c. (50 PFU/mouse); on day 5 postinfection, mice were sacrificed and the virus titers in the brain and liver determined. (C) Mice ($n = 5$) were infected i.h. (500 PFU/mouse), and the virus titer in the liver on day 5 postinfection was determined. The dashed lines represent the limit of detection, and the error bars represent the standard error of the mean (SEM) (***, $P < 0.001$). (D) Liver sections from mice ($n = 3$) sacrificed on day 5 postinfection were stained with hematoxylin and eosin. One representative section is shown. The data are from one representative experiment of two.

domain as well as a 1-amino-acid substitution, L48R, within the receptor-binding domain at the amino terminus of the S1 subunit (Table 1). To address whether this deletion and mutation affect liver tropism, we exchanged the spike genes of rSD and rWU to generate rSD.S_{WU} and rWU.S_{SD} (Fig. 3A) and characterized their growth kinetics in L2 cells. Compared to rSD, rSD.S_{WU} replicated to a 10- to 100-fold-higher titer in L2 cells, suggesting that spike substitution enhanced virus production *in vitro* (Fig. 3B). Consistent with these data, rWU.S_{SD} displayed a 10- to 100-fold-lower titer than rWU (Fig. 3D). In contrast to the *in vitro* results, while both rSD.Swu and rSD failed to replicate in the liver in B6 mice (Fig. 3C), rWU and rWU.S_{SD} replicated to similar titers in the liver in B6 mice (Fig. 3E). Thus, while the spike protein does influence replication kinetics *in vitro*, spike is not a significant determinant of WU liver tropism.

The 3′ JHM.WU genome fragments F and G, encoding some of the nonstructural proteins and all of the structural proteins, enable JHM.SD to replicate in the liver. After finding that the JHM.WU spike protein did not enhance rSD replication in the liver, we investigated which other structural and/or nonstructural proteins might play a role in liver tropism. Thus, we replaced the F and/or G fragment(s) of JHM.SD with the corresponding fragment(s) of JHM.WU to generate rSD.Gwu, rSD.F_{wu}, and rSD.$F_{WU}G_{WU}$ (Fig. 4A). The G fragment encodes most of the structural proteins, including the nucleocapsid, membrane protein (M), small membrane protein (E), spike, and part of the HE protein (Fig. 1); the F fragment encodes the rest of the HE protein, accessory protein ns2, and a segment of open reading frame (ORF) 1b including the carboxy-terminal portion of replicase protein nsp12 as well as all of nsp13 to -16. Replacement of the G fragment alone or in combination with F conferred efficient replication in L2 cells *in vitro*, while rSD.F_{WU} did not replicate to a higher titer than rSD (Fig. 4B). In contrast, *in vivo*, replacement of either the F or G fragment alone only marginally increased rSD replication in the liver at 5 days postinfection. However, replacement of both the F and G fragments (rSD.$F_{WU}G_{WU}$) restored replication to approxi-

TABLE 1 Amino acid differences between JHM.SD and JHM.WU encoded proteins[a]

Fragment[b]	Protein[c]	Amino acid position[d]	JHM.SD	JHM.WU
A	nsp1	194	R	K
	nsp2	282	V	L
		326	A	V
	nsp3	173	P	H
C	nsp5	262	M	V
	nsp6	21	F	V
F	nsp13	335	V	A
	nsp15	41	E	V
	ns2	177	D	G
	HE	3	R	S
G	HE	408	I	V
		425	M	I
		426	F	L
	Spike	48	L	R
		454–594		Deletion[e]
	M	155	L	F
		224	A	V

[a] GenBank accession numbers: JHM.SD (RJHM/A), FJ647219.1; JHM.WU (wb-3), JX169867.1.
[b] Fragments A, C, F, and G encoded amino acid differences between JHM.SD and JHM.WU.
[c] Proteins that contain amino acid polymorphisms are listed.
[d] The position of the amino acid variation in each protein is shown.
[e] JHM.WU spike protein contains a 141-amino-acid deletion relative to JHM.SD spike.

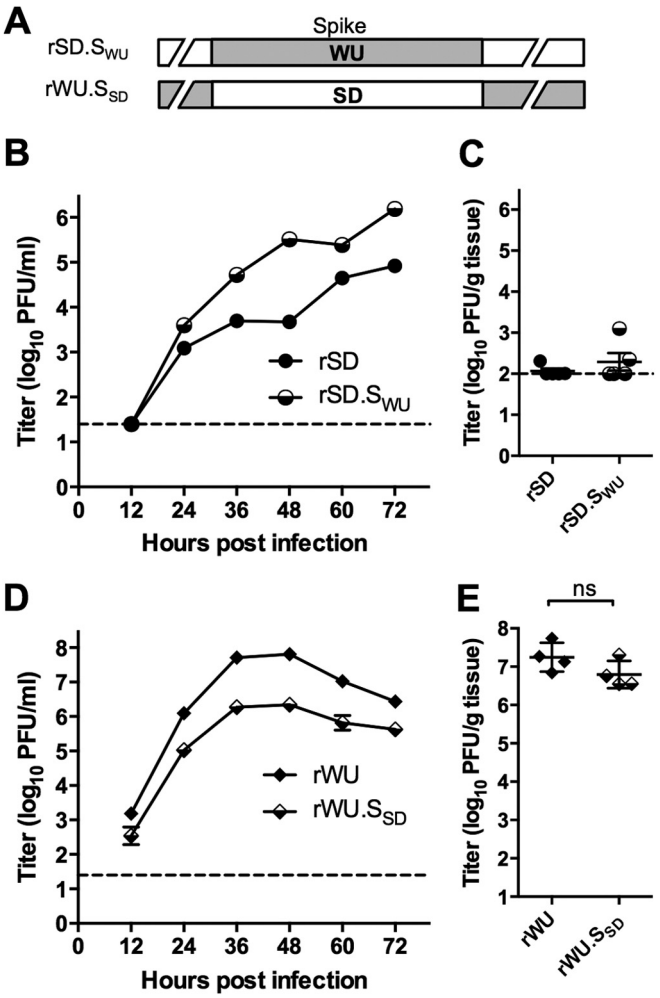

FIG 3 Replication of spike-exchanged recombinant viruses *in vitro* and *in vivo*. (A) Schematic diagram of recombinant viral genomes with exchanged spike genes. (B and D) L2 cells were infected (in triplicate, MOI = 0.01 PFU/cell) with rSD and rSD.S_{WU} (B) or rWU and rWU.S_{SD} (D), and the supernatant was collected at the indicated time points postinfection for determination of the viral titer. (C and E) Mice ($n = 4$ or 5) were infected i.h. with 500 PFU/mouse of rSD and rSD.S_{WU} (C) or rWU and rWU.S_{SD} (E) and were sacrificed on day 5 postinfection, and the viral titer in the liver was determined. The dashed lines represent the limit of detection. The error bars represent the SEM (ns, nonsignificant). The data are from one representative experiment of two.

mately 2.6×10^5 PFU g^{-1} in the liver, about 10- to 50-fold lower than that for rWU (Fig. 4C).

The JHM.SD nsp13 and M protein sequences attenuate JHM.WU replication *in vitro* and in the liver. To identify which protein(s) encoded within fragments F and G of JHM.WU is essential to MHV liver replication, we compared the sequences of the proteins encoded by fragments F and G between the two JHM strains (Table 1). In addition to the differences in the spike, discussed above, these included amino acid substitutions in the structural proteins HE and M (fragment G) and the accessory protein ns2 and nonstructural replicase proteins nsp13 and nsp15 (fragment F) (26) (Fig. 5A). To evaluate the importance of these polymorphisms, we generated recombinant viruses in the JHM.WU background bearing amino acid substitutions found in the JHM.SD genome (Fig. 5A). Four of these, rWU.HE^{V408I}, rWU.HE^{I425M,L426F}, rWU.ns2^{G177D}/HE^{S3R}, and rWU.nsp15^{V41E}, exhibited growth kinetics in L2 cells that were similar to those of rWU (Fig. 5B and C) and furthermore replicated as efficiently (i.e., with no significant difference) as rWU in mouse liver (Fig. 5C and E). (The *P* value for nsp15 versus wt rWU mouse liver replication is 0.0952.) Therefore, the sequence differences in HE, ns2, and nsp15 in the JHM.SD genome did not significantly affect viral replication in the liver.

In contrast, mutations within the M and nsp13 genes conferred phenotypic changes *in vitro* and *in vivo*. Two amino acid differences were identified between M proteins of JHM.WU and JHM.SD (Table 1). To determine their impact on viral replication, we generated recombinant viruses with each or both of the JHM.SD M substitutions in the rWU background. The recombinant viruses containing single substitutions (rWU.M^{F155L} and rWU.M^{V224A}) did not replicate significantly differently from rWU *in vitro* (Fig. 5B) or *in vivo* (Fig. 5C). However, the double mutant rWU.M^{F155L,V224A} showed impaired viral growth kinetics in L2 cells (Fig. 5B), and, likely as a consequence of less robust replication, an approximately 1,000-fold decrease in the viral load in the livers of infected mice compared to rWU (Fig. 5C). Similarly, the nsp13 gene of rWU also contributed to efficient replication *in vitro* and *in vivo*. rWU.nsp13^{A335V}, encoding the nsp13 of JHM.SD, displayed attenuated growth kinetics in L2 cells relative to rWU as well as an approximately 30-fold lower viral titer in the livers of infected mice. Thus, sequences in the M and nsp13 proteins of JHM.WU were responsible for the enhanced replication of rSD.$F_{WU}G_{WU}$ in the liver.

nsp1 does not affect replication in L2 cells *in vitro* but influences viral replication in the liver. As described above, fragments F and G were insufficient for restoring rSD replication in the liver to the level of rWU, and there were no amino acid differences between the fragment B-, D-, and E-encoded proteins of JHM.SD and JHM.WU. These data suggested that WU fragment(s) A and/or C was likely to contribute to liver replication. To test this, we generated chimeric viruses in the rWU background in which fragment A or C was replaced with the corresponding JHM.SD fragment (Fig. 6A). Both rWU.C_{SD} and rWU.A_{SD} showed growth kinetics similar to those of rWU in L2 cells; however, rWU.A_{SD} was also significantly attenuated (approximately 100-fold) for replication in the liver (Fig. 6B and C). Four amino acid differences between JHM.WU and JHM.SD were identified in the A fragment (nsp1, nsp2, and nsp3), and mutations corresponding to these differences were introduced into the rWU genome to generate rWU.nsp1^{K194R}, rWU.nsp2^{L282V}, rWU.nsp2^{V326A}, and rWU.nsp3^{H173P} (Fig. 6A). All four viruses replicated with similar kinetics and to a similar final titer as rWU *in vitro* in L2 cells (Fig. 6B), indicating that polymorphisms in nsp1, nsp2, or nsp3 had no detectable effect on *in vitro* replication.

While there were no detectable effects on liver replication observed during infection with nsp2 or nsp3 mutants, attenuation of liver replication (approximately 100-fold) was observed in mice infected with rWU.nsp1^{K194R} compared with rWU (Fig. 6C). rWU.nsp1^{K194R} replicated in the liver to a similar extent as rWU.A_{SD} and rSD.$F_{WU}G_{WU}$ (which contains fragments A through E from rSD), indicating that the nsp1 amino acid substitution alone is sufficient to account for the attenuation (relative to rWU) of the latter two chimeric viruses. To further investigate the impact of nsp1 residue 194 on pathogenesis, the reverse substitution was introduced into the rSD genome to generate rSD.nsp1^{R194K}. Sim-

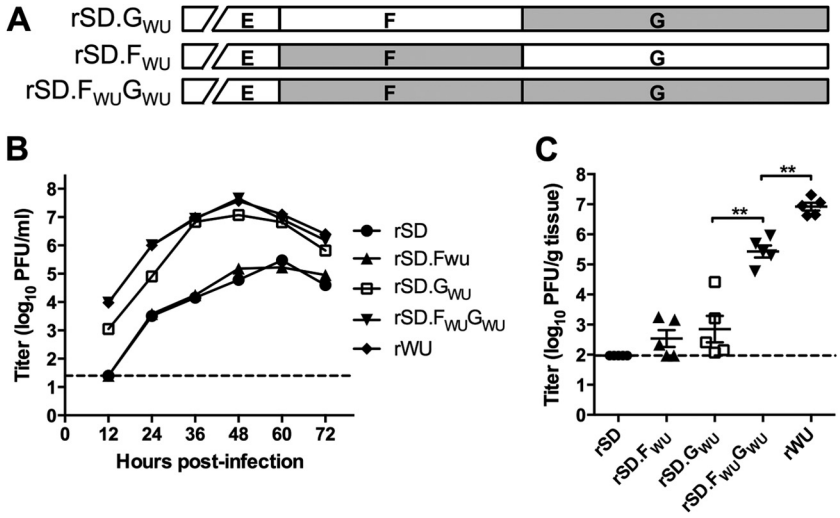

FIG 4 Partial restoration of the replication of chimeric rSD viruses in the liver by replacement of F and/or G fragments with those of rWU. (A) Schematic diagram of the chimeric rSD viruses expressing the F or/and G fragment of rWU. (B) L2 cells were infected (in triplicate, MOI = 0.01 PFU/cell) and supernatants collected at the indicated time points postinfection for determination of the viral titer. (C) Mice ($n = 5$) were infected i.h. (500 PFU/mouse) and sacrificed on day 5 postinfection, and the viral titer in the liver was determined. The dashed line represents the limit of detection. The error bars represent the SEM (**, $P < 0.01$). The data are from one representative experiment of two.

ilar *in vitro* growth kinetics was observed for rSD.nsp1^{R194K} and rSD in L2 cells (Fig. 6D). However, rSD.nsp1^{R194K} replicated to a significantly higher titer in mouse liver (Fig. 6E) (rSD was undetectable, as in previous figures). As the nsp1 residue K194 is conserved among all MHV strains except JHM.SD (see Fig. 8 and Discussion), the same K194R substitution was introduced into the genome of recombinant A59 (rA59), another hepatotropic strain used frequently for MHV pathogenesis studies, to generate A59.nsp1^{K194R}. The A59.nsp1^{K194R} mutant replicated similarly to rA59 *in vitro* but showed attenuated (near 100-fold) liver replication (Fig. 6F and G). To further understand the impact of mutations in nsp1, we constructed mutant virus A59.nsp1$^{R193S/K194E}$ with substitutions introducing charge alterations into nsp1, analogous to a SARS nps1 reported in the literature (27). However, the double mutant had a phenotype similar to that of the single mutant A59.nsp1^{K194R} in terms of replication both *in vitro* in L2 cells and *in vivo* in the liver (Fig. 6F and G). Moreover, the same double substitution was introduced into nsp1 of rWU (rWU.nsp1$^{R193S/K194E}$); as for rA59, no difference was observed between the single and double mutants in replication in either L2 cells or the liver (data not shown). These data suggest that mutation of the conserved K194 decreases virulence without affecting *in vitro* replication.

The nsp1 protein antagonizes IFN-β production during MHV infection. Previous studies showed that the MHV nsp1 protein might be involved in antagonizing the type I IFN immune response (27, 28). To investigate whether the IFN response may be involved in the phenotype of our nsp1 mutants, we compared the replication as well as the IFN-β production of both rWU and rA59 with those of their respective nsp1^{K194R} mutants in bone marrow-derived macrophages (BMM), one of the few cell types in which MHV elicits a type I IFN response (29, 30). The rA59.nsp1^{K194R} and A59.nsp1$^{R193S/K194E}$ mutants replicated similarly, albeit to a 6- to 10-fold-lower titer than for rA59 by 24 h postinfection (Fig. 7A). However, the replication of both mutants was restored in the absence of IFN signaling, i.e., during replication in BMM derived from IFNAR$^{-/-}$ mice (Fig. 7B). A similar pattern was observed for induction of IFN-β expression upon infection: BMM infected with wt rA59 produced approximately 210 pg ml^{-1} of IFN-β in the culture supernatant, whereas those infected with the rA59.nsp1^{K194R} mutant produced 3,000 pg ml^{-1} of IFN-β, presumably resulting in more robust antiviral activity. Interestingly, the effects of these mutations were less pronounced in the rWU background. We observed no difference in replication between rWU and either rWU-nsp1^{K194R} or rWU.nsp1$^{R193S/K194E}$ (Fig. 7D), and the difference in IFN-β production was also smaller (Fig. 7F): while BMM infected with rWU produced no detectable IFN-β in the culture supernatant, those infected with rWU-nsp1^{K194R} produced 140 pg ml^{-1} (Fig. 7F). Consistent with these findings, BMM infected with rSD-nsp1^{R194K} induced 12-fold less IFN-β than those infected with wt rSD (Fig. 7G). Thus, the conserved nsp1 K194 residue found in the hepatotropic rWU and rA59, while not important for replication in the L2 cell line *in vitro*, was associated with lower IFN-β production in BMM as well as higher liver titers.

DISCUSSION

Infection of mice with laboratory strains of MHV causes hepatitis and encephalitis in a strain-specific manner. JHM.SD and JHM.WU are very closely related isolates with strikingly different *in vitro* replication and *in vivo* hepatovirulence phenotypes, likely reflecting the passage history of the two isolates since their derivation from the same JHM isolate, which had been brain adapted by many serial passage through suckling mouse brains (31). MHV-4 (from which recombinant JHM.SD was derived) was plaque purified from the mouse brain-passaged virus, while JHM.WU (wb-3) was serially passaged 20 times in tissue culture before plaque purification (5, 15, 16, 32). The passage history coupled with data presented here suggest that adaptation to mouse brain may select for variants unable to replicate efficiently in tissue culture or in the liver. This is consistent with our previous work in

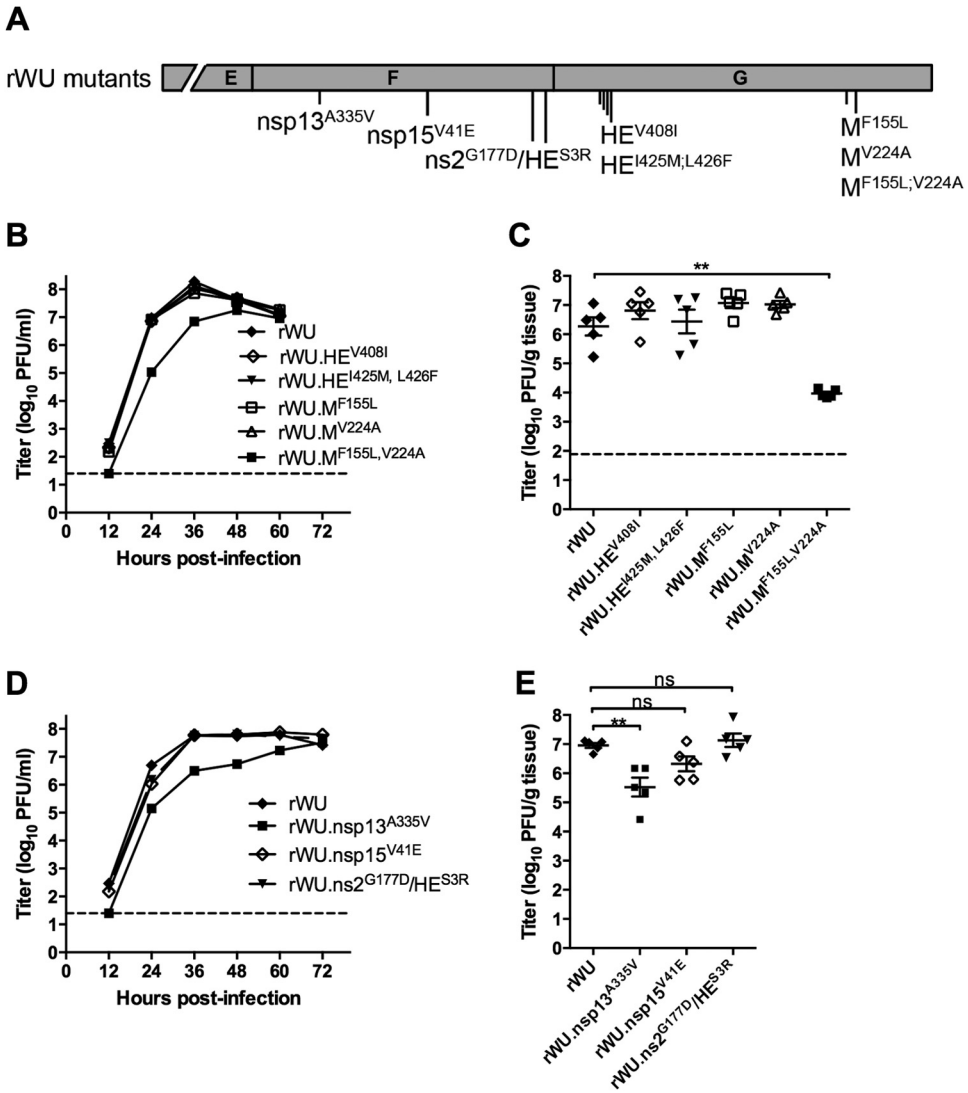

FIG 5 Amino acid substitutions in the nsp13 and M proteins attenuate rWU replication. (A) Schematic diagram of the rWU genome showing the amino acid differences from JHM.SD in the F and G fragments. (B and D) L2 cells were infected (in triplicate, MOI = 0.01 PFU/cell) with viruses with mutations in the G fragment (B) or F fragment (D), and supernatant was collected at the indicated times postinfection for determination of the virus titer. (C and E) B6 mice (n = 5) were infected i.h. (500 PFU/mouse) with viruses with mutations in the G fragment (C) or F fragment (E). On day 5 postinfection, the mice were sacrificed and the virus titer in the liver determined. The dashed lines represent the limit of detection. The error bars represent the SEM (ns, nonsignificant; **, $P < 0.01$). The data are from one representative experiment of two.

which nonhepatotropic variants of rA59 were selected by passage in primary glial cell cultures (22, 23).

Using reverse genetic systems, we constructed chimeric recombinant viruses and used them to identify the JHM.WU-encoded determinants of efficient replication in tissue culture and of liver pathogenesis. There were remarkably few amino acid differences between the proteins encoded by these two viruses. The 3′ third of the JHM.WU genome, encoding the structural proteins, was necessary for efficient *in vitro* replication, whereas replication to a high titer in the liver was multifactorial and mapped to amino acid substitutions in the membrane (M) structural protein as well as in nonstructural replicase proteins (nsp1 and nsp13) (27, 28, 33).

We initially hypothesized that the spike protein, which is responsible for receptor binding and viral entry, would define the difference in tropism between JHM.SD and JHM.WU. Indeed, numerous past studies demonstrated that sequences in several domains of the MHV spike impact tropism and virulence (8, 16, 34–37). The high neurovirulence of JHM.SD has been associated with the long hypervariable domain in the S1 subunit of the JHM spike protein (7, 34). Surprisingly, JHM.WU is highly neurovirulent despite the 141-amino-acid deletion in the hypervariable domain, and our data indicate that the JHM.WU spike does not confer hepatotropism; although the JHM.WU spike enhanced replication of rSD.S_{WU} to some extent in cell culture (Fig. 3B and D), there was no significant effect on replication in the liver (Fig. 3C and E). Similarly, a chimeric rSD expressing the spike of hepatotropic MHV-A59 was not able to replicate in the liver (13). These results indicated that MHV replication in the liver is largely determined by postentry events and that attenuation of

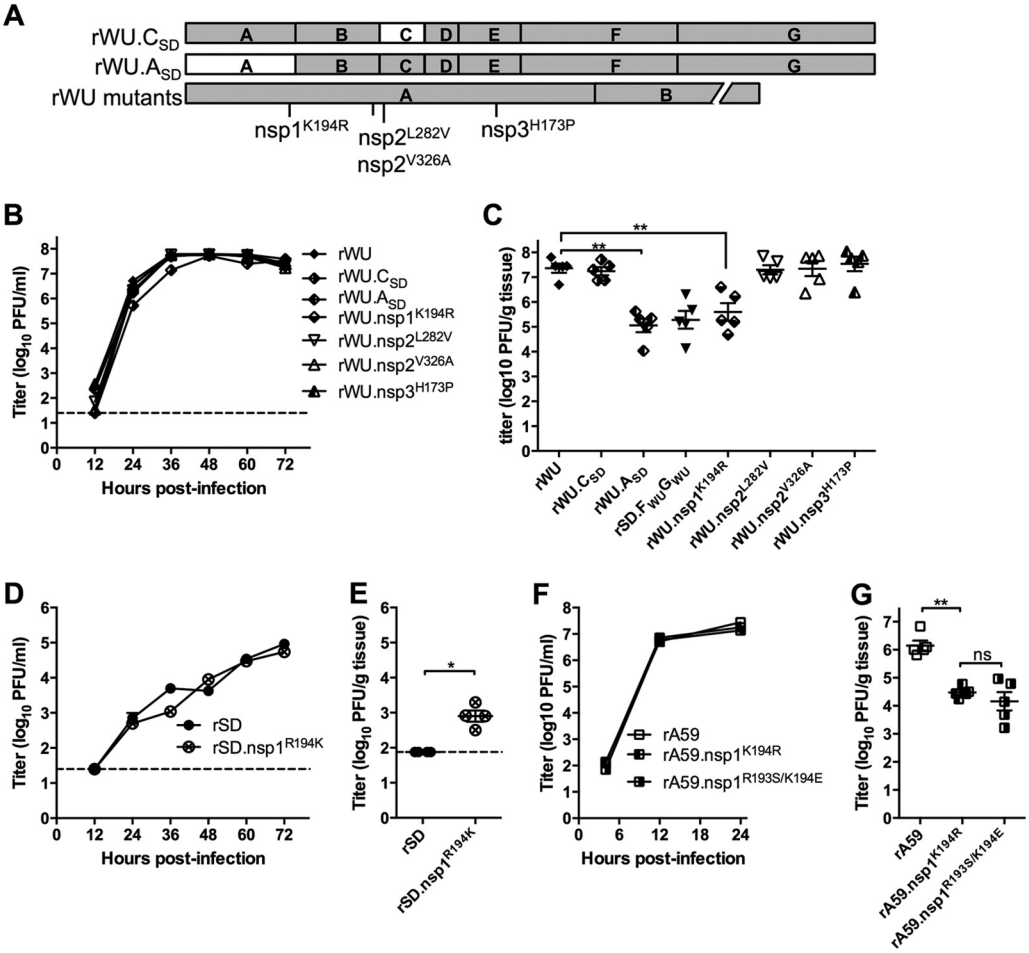

FIG 6 A single amino acid substitution in nsp1 attenuates the replication of rWU and rA59 in the liver. (A) Schematic diagram of the chimeric rWU viruses with the C or A fragment of rSD or with point substitutions in the A fragment. (B, D, and F) L2 cells were infected (in triplicate) at an MOI of 0.01 PFU/cell for the rWU background viruses or 1 PFU/cell for the rA59 background viruses, and supernatant was collected at the indicated times postinfection for determination of the viral titer. (C, E, and G) Mice ($n = 5$) were infected i.h. with 500 PFU/mouse for the rWU background viruses and rSD.$F_{WU}G_{WU}$ (C), 10,000 PFU/mouse for the rSD viruses (E), or 5,000 PFU/mouse for the rA59 background viruses (G). On day 5 postinfection, mice were sacrificed and the viral titer in the liver was determined. The dashed lines represent the limit of detection. The error bars represent the SEM (ns, nonsignificant; *, $P < 0.05$; **, $P < 0.01$). The data are from one representative experiment of two.

replication *in vitro* may not predict poor viral replication *in vivo*. Interestingly, while JHM.SD replicates poorly *in vitro* and minimally in the liver, it replicates well in the central nervous system, where it spreads extensively and efficiently throughout the brain, in multiple cell types, even in the absence of the only known MHV receptor, CEACAM1a (38, 39). While difficult to explain on a mechanistic level, this likely reflects a very strong selection for the ability to replicate in the brain resulting from serial brain passage.

The membrane protein (M), the most abundant component of the virion, is key to viral particle assembly through interactions with spike (40) and nucleocapsid (41) as well as M-M interactions (42) and may, in addition, interact with the viral RNA (43, 44) through the carboxy-terminal tail of the protein. Consistent with the role of M in virus assembly, an M protein mutant of SARS-CoV, selected by serial passage in primary human renal tubular epithelial cells, was associated with persistent infection and enhanced virus production (45). The combined introduction of two JHM.SD amino acid substitutions together into the carboxy-terminal endodomain of rWU M protein (rWU.M^{F155L,V224A}) impaired replication in L2 cells and quite dramatically in the mouse liver, although neither substitution alone conferred any detectable phenotype (Fig. 5). While rWU.M^{F155L,V224A} replicated moderately less well than rWU in L2 cells, it was about 1,000-fold attenuated in the liver, suggesting that other virus-host interactions in addition to virus assembly were contributing to the loss of replication in the liver. Interestingly, a study of MHV-A59 M protein glycosylation variants correlated replication in the liver with induction of type I interferon (46). Future studies will address whether mutations within M (as well as nsp1 [discussed below]) contribute to the differences observed in IFN production during JHM.SD versus JHM.WU infection of BMM (Fig. 7F and G).

We also identified amino acid differences between the JHM.SD and JHM.WU genomes within nonstructural proteins (Table 1). Among these, only the JHM.SD-specific amino acid substitutions in nsp1 and nsp13 influenced the phenotype. Introduction of an A335V substitution into the helicase domain of

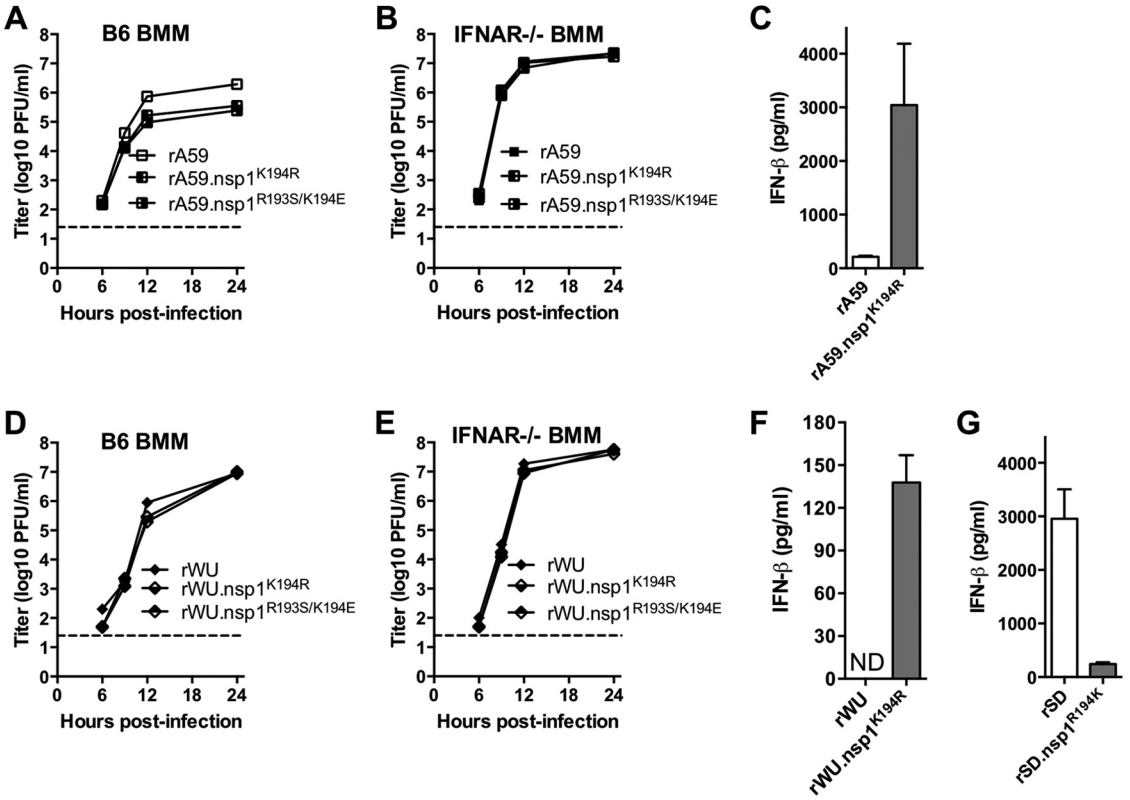

FIG 7 nsp1 antagonizes IFN-β production. BMM derived from B6 (A and D) or IFNAR$^{-/-}$ (B and E) mice were infected (MOI = 1 PFU/cell) with each virus, and supernatant was collected at the indicated time points postinfection for determination of the viral titer. B6 BMM were infected (MOI = 2 PFU/cell [C and F] and 1 PFU/cell [G]) with the indicated viruses, and at 24 h postinfection, IFN-β protein in the B6 BMM supernatants was quantified by ELISA. The dashed lines represent the limit of detection. The data are from one representative experiment of two (each performed in triplicate). ND, not detectable.

JHM.WU nsp13 attenuates viral replication both *in vitro* and *in vivo* (47) (Fig. 5). As the A335V substitution confers less efficient replication *in vitro*, it is likely that the *in vivo* effects are due to less efficient replication. Consistent with a role of nsp13 in contributing to efficient replication, nsp13 mutations were identified during the emergence of SARS-CoV into the human population and in mouse-adapted strains, which replicate more efficiently in the lung (48, 49).

Nsp1 is the N-terminal cleavage product of the replicase polyprotein and is encoded by all betacoronaviruses. While nsp1 varies in length, from 247 residues in MHV to 175 in bat CoV-HKU9, certain regions are conserved (20). The K194 residue of MHV nsp1 is located in a positively charged domain (LLRK^{194}GGNKG), is relatively conserved among betacoronaviruses (Fig. 8), and is presumed to be involved in RNA binding and/or protein-protein interactions (50, 51). The K194 residue of MHV nsp1 is conserved among all MHV isolates except JHM.SD (with its K194R substitution) and also throughout other betacoronaviruses (Fig. 8). We

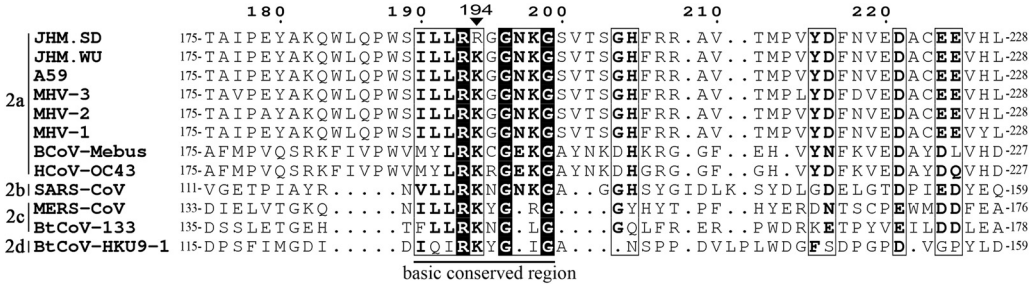

FIG 8 Sequence alignment of the *Betacoronavirus* nsp1 region surrounding lysine 194. nsp1 sequences of the representative *Betacoronavirus* strains from subgroup 2a through 2d were aligned using CLUSTAL 2.1. Completely conserved residues are in black boxes, and partially conserved residues are in white boxes. The positively charged conserved domain is underlined, and MHV residue 194 is indicated by the black triangle. GenBank accession numbers are as follows: JHM.SD (RJHM/A), FJ647219.1; JHM.WU (wb-3), JX169867.1; A59 (RA59/R13), FJ647218.1; MHV-3, FJ647224.1; MHV-2, AF201929.1; MHV-1, FJ647223.1; BCoV-Mebus (bovine coronavirus Mebus strain), U00735.2; HCoV-OC43 (human coronavirus OC43), NC_005147.1; SARS-CoV (SARS coronavirus CFB/SZ/94/03), AY545919.1; MERS-CoV (MERS coronavirus EMC/2012), JX869059.2; BtCoV-133 (bat coronavirus 133/2005), NC_008315.1; BtCoV-HKU9-1 (bat coronavirus HKU9-1), NC_009021.1.

found that neither K194R nor the charge-disrupting R193S/K194E double substitution within JHM.WU had a detectable effect on replication *in vitro*; however, both substitutions conferred approximately 100-fold attenuated replication *in vivo*. Introduction of the K194R or R193S/K194E substitutions into another hepatotropic strain, rA59, had similar attenuating effects on liver replication. Conversely, the R194K substitution in the nsp1 of rSD confers a detectable albeit low level of virus replication in the liver.

Previous studies have reported an impaired and delayed type I interferon (IFN) response during *in vitro* infection by MHV, SARS-CoV, or MERS-CoV (52–55) and that this may in part be conferred by nsp1 (20). Data from our lab suggested that MHV-A59 inhibits IFN protein production at the translational level (53). In other studies, MHV-A59 mutants either with a deletion of the $LLRK^{194}GGNKG$ domain (56) or with an internal downstream 33-amino-acid in-frame deletion (28) were attenuated for liver replication as well as the onset of hepatitis in wild-type mice, while the latter deletion mutant recovered replication in type I IFN receptor expression-deficient ($IFNAR^{-/-}$) mice (28). In addition, transient expression of MHV or SARS-CoV nsp1 significantly reduced expression of a luciferase reporter gene under the control of the IFN-β or IFN-stimulated response element (ISRE) promoter (28), implying that nsp1 may antagonize the type I interferon signaling pathway. Furthermore, the importance of residues R193/K194 for virulence via IFN antagonism is supported by the finding that a SARS-CoV mutant expressing nsp1 with amino acid substitutions of these conserved residues (R124S/K125E, corresponding to residues 193/194 of MHV nsp1) was more sensitive than wt virus to type I IFN treatment (27). In another group of studies, the nsp1 of SARS-CoV was reported to promote mRNA degradation and to inhibit protein translation, thereby inhibiting IFN-β production at both the mRNA and protein levels (33, 57–60), while an nps1 mutant (R124A/K125A) was unable to degrade mRNA but retained the ability to inhibit protein synthesis. Thus, the effects of nsp1 on transcription and translation are complex and may be coronavirus strain type dependent (20).

Interestingly, the attenuation phenotype conferred by mutation of nsp1 is observed only in the livers of infected mice and not in the brains. In our studies following intracranial infection, while $rWU.nsp1^{K194}$ was significantly attenuated for liver replication compared to rWU, there were no significant differences observed in replication of the two viruses in the brain (data not shown). This is similar to the phenotype of an A59 ns2 PDE mutant, which replicates robustly in the brain while being highly attenuated for liver replication and hepatitis (12, 30). The liver-specific attenuation of these mutants, both deficient in type I IFN antagonism, is likely explained by our previous finding that basal levels of interferon-stimulated gene expression are much higher in the liver than in the brain, leading to a more robust host innate response in the liver than in the brain (14, 30) The mechanism by which MHV nsp1 interferes with the type I IFN response and its role in liver tropism are not yet well understood and will be a subject of further investigation.

Elucidating the mechanisms underlying tropism and virulence using these model coronaviruses may also contribute to our knowledge of the pathogenesis of the human-pathogenic coronaviruses such as SARS-CoV or MERS-CoV, as the LRKGGNKG motif of nsp1 as well as the nsp13 helicase and M protein are conserved among these viruses. Understanding these virulence determinants may in the long term contribute to the design of live attenuated vaccines for coronaviruses.

ACKNOWLEDGMENTS

This work was supported by NIH grants R01-NS081008 and R56-AI095285 (S.R.W.) and U19 AI109761 (R.S.B.). T.J.C. was supported in part by training grant T32-AI007324 and J.M.P. by grant K08-AI098503.

REFERENCES

1. **Cavanagh D.** 1997. Nidovirales: a new order comprising Coronaviridae and Arteriviridae. Arch Virol **142:**629–633.
2. **Graham RL, Donaldson EF, Baric RS.** 2013. A decade after SARS: strategies for controlling emerging coronaviruses. Nat Rev Microbiol **11:**836–848. http://dx.doi.org/10.1038/nrmicro3143.
3. **Song D, Park B.** 2012. Porcine epidemic diarrhoea virus: a comprehensive review of molecular epidemiology, diagnosis, and vaccines. Virus Genes **44:**167–175. http://dx.doi.org/10.1007/s11262-012-0713-1.
4. **Navas-Martin S, Weiss SR.** 2003. SARS: lessons learned from other coronaviruses. Viral Immunol **16:**461–474. http://dx.doi.org/10.1089/088282403771926292.
5. **Weiss SR, Leibowitz JL.** 2011. Coronavirus pathogenesis. Adv Virus Res **81:**85–164. http://dx.doi.org/10.1016/B978-0-12-385885-6.00009-2.
6. **Navas-Martin S, Hingley ST, Weiss SR.** 2005. Murine coronavirus evolution in vivo: functional compensation of a detrimental amino acid substitution in the receptor binding domain of the spike glycoprotein. J Virol **79:**7629–7640. http://dx.doi.org/10.1128/JVI.79.12.7629-7640.2005.
7. **Parker SE, Gallagher TM, Buchmeier MJ.** 1989. Sequence analysis reveals extensive polymorphism and evidence of deletions within the E2 glycoprotein gene of several strains of murine hepatitis virus. Virology **173:**664–673. http://dx.doi.org/10.1016/0042-6822(89)90579-5.
8. **Gallagher TM, Escarmis C, Buchmeier MJ.** 1991. Alteration of the pH dependence of coronavirus-induced cell fusion: effect of mutations in the spike glycoprotein. J Virol **65:**1916–1928.
9. **Tsai JC, de Groot L, Pinon JD, Iacono KT, Phillips JJ, Seo SH, Lavi E, Weiss SR.** 2003. Amino acid substitutions within the heptad repeat domain 1 of murine coronavirus spike protein restrict viral antigen spread in the central nervous system. Virology **312:**369–380. http://dx.doi.org/10.1016/S0042-6822(03)00248-4.
10. **Eriksson KK, Cervantes-Barragan L, Ludewig B, Thiel V.** 2008. Mouse hepatitis virus liver pathology is dependent on ADP-ribose-1-phosphatase, a viral function conserved in the alpha-like supergroup. J Virol **82:**12325–12334. http://dx.doi.org/10.1128/JVI.02082-08.
11. **Fehr AR, Athmer J, Channappanavar R, Phillips JM, Meyerholz DK, Perlman S.** 2015. The NSP3 macrodomain promotes virulence in mice with coronavirus-induced encephalitis. J Virol **89:**1523–36. http://dx.doi.org/10.1128/JVI.02596-14.
12. **Zhao L, Jha BK, Wu A, Elliott R, Ziebuhr J, Gorbalenya AE, Silverman RH, Weiss SR.** 2012. Antagonism of the interferon-induced OAS-RNase L pathway by murine coronavirus ns2 protein is required for virus replication and liver pathology. Cell Host Microbe **11:**607–616. http://dx.doi.org/10.1016/j.chom.2012.04.011.
13. **Navas S, Weiss SR.** 2003. Murine coronavirus-induced hepatitis: JHM genetic background eliminates A59 spike-determined hepatotropism. J Virol **77:**4972–4978. http://dx.doi.org/10.1128/JVI.77.8.4972-4978.2003.
14. **Zhao L, Rose KM, Elliott R, Van Rooijen N, Weiss SR.** 2011. Cell-type-specific type I interferon antagonism influences organ tropism of murine coronavirus. J Virol **85:**10058–10068. http://dx.doi.org/10.1128/JVI.05075-11.
15. **Schwarz B, Routledge E, Siddell SG.** 1990. Murine coronavirus nonstructural protein ns2 is not essential for virus replication in transformed cells. J Virol **64:**4784–4791.
16. **Dalziel RG, Lampert PW, Talbot PJ, Buchmeier MJ.** 1986. Site-specific alteration of murine hepatitis virus type 4 peplomer glycoprotein E2 results in reduced neurovirulence. J Virol **59:**463–471.
17. **Yount B, Denison MR, Weiss SR, Baric RS.** 2002. Systematic assembly of a full-length infectious cDNA of mouse hepatitis virus strain A59. J Virol **76:**11065–11078. http://dx.doi.org/10.1128/JVI.76.21.11065-11078.2002.
18. **Sperry SM, Kazi L, Graham RL, Baric RS, Weiss SR, Denison MR.** 2005. Single-amino-acid substitutions in open reading frame (ORF) 1b-nsp14

and ORF 2a proteins of the coronavirus mouse hepatitis virus are attenuating in mice. J Virol **79:**3391–3400. http://dx.doi.org/10.1128/JVI.79.6.3391-3400.2005.
19. **Roth-Cross JK, Stokes H, Chang G, Chua MM, Thiel V, Weiss SR, Gorbalenya AE, Siddell SG.** 2009. Organ-specific attenuation of murine hepatitis virus strain A59 by replacement of catalytic residues in the putative viral cyclic phosphodiesterase ns2. J Virol **83:**3743–3753. http://dx.doi.org/10.1128/JVI.02203-08.
20. **Narayanan K, Ramirez SI, Lokugamage KG, Makino S.** 26 November 2014. Coronavirus nonstructural protein 1: common and distinct functions in the regulation of host and viral gene expression. Virus Res http://dx.doi.org/10.1016/j.virusres.2014.11.019.
21. **Ontiveros E, Kuo L, Masters PS, Perlman S.** 2001. Inactivation of expression of gene 4 of mouse hepatitis virus strain JHM does not affect virulence in the murine CNS. Virology **289:**230–238. http://dx.doi.org/10.1006/viro.2001.1167.
22. **Hingley ST, Gombold JL, Lavi E, Weiss SR.** 1994. MHV-A59 fusion mutants are attenuated and display altered hepatotropism. Virology **200:**1–10. http://dx.doi.org/10.1006/viro.1994.1156.
23. **Gombold JL, Hingley ST, Weiss SR.** 1993. Fusion-defective mutants of mouse hepatitis virus A59 contain a mutation in the spike protein cleavage signal. J Virol **67:**4504–4512.
24. **Navas-Martin S, Brom M, Chua MM, Watson R, Qiu Z, Weiss SR.** 2007. Replicase genes of murine coronavirus strains A59 and JHM are interchangeable: differences in pathogenesis map to the 3′ one-third of the genome. J Virol **81:**1022–1026. http://dx.doi.org/10.1128/JVI.01944-06.
25. **MacNamara KC, Chua MM, Phillips JJ, Weiss SR.** 2005. Contributions of the viral genetic background and a single amino acid substitution in an immunodominant CD8+ T-cell epitope to murine coronavirus neurovirulence. J Virol **79:**9108–9118. http://dx.doi.org/10.1128/JVI.79.14.9108-9118.2005.
26. **Snijder EJ, Bredenbeek PJ, Dobbe JC, Thiel V, Ziebuhr J, Poon LL, Guan Y, Rozanov M, Spaan WJ, Gorbalenya AE.** 2003. Unique and conserved features of genome and proteome of SARS-coronavirus, an early split-off from the coronavirus group 2 lineage. J Mol Biol **331:**991–1004. http://dx.doi.org/10.1016/S0022-2836(03)00865-9.
27. **Wathelet MG, Orr M, Frieman MB, Baric RS.** 2007. Severe acute respiratory syndrome coronavirus evades antiviral signaling: role of nsp1 and rational design of an attenuated strain. J Virol **81:**11620–11633. http://dx.doi.org/10.1128/JVI.00702-07.
28. **Zust R, Cervantes-Barragan L, Kuri T, Blakqori G, Weber F, Ludewig B, Thiel V.** 2007. Coronavirus non-structural protein 1 is a major pathogenicity factor: implications for the rational design of coronavirus vaccines. PLoS Pathog **3:**e109. http://dx.doi.org/10.1371/journal.ppat.0030109.
29. **Roth-Cross JK, Bender SJ, Weiss SR.** 2008. Murine coronavirus mouse hepatitis virus is recognized by MDA5 and induces type I interferon in brain macrophages/microglia. J Virol **82:**9829–9838. http://dx.doi.org/10.1128/JVI.01199-08.
30. **Zhao L, Birdwell LD, Wu A, Elliott R, Rose KM, Phillips JM, Li Y, Grinspan J, Silverman RH, Weiss SR.** 2013. Cell-type-specific activation of the oligoadenylate synthetase-RNase L pathway by a murine coronavirus. J Virol **87:**8408–8418. http://dx.doi.org/10.1128/JVI.00769-13.
31. **Weiner LP.** 1973. Pathogenesis of demyelination induced by a mouse hepatitis. Arch Neurol **28:**298–303. http://dx.doi.org/10.1001/archneur.1973.00490230034003.
32. **Bender SJ, Weiss SR.** 2010. Pathogenesis of murine coronavirus in the central nervous system. J Neuroimmune Pharmacol **5:**336–354. http://dx.doi.org/10.1007/s11481-010-9202-2.
33. **Kamitani W, Narayanan K, Huang C, Lokugamage K, Ikegami T, Ito N, Kubo H, Makino S.** 2006. Severe acute respiratory syndrome coronavirus nsp1 protein suppresses host gene expression by promoting host mRNA degradation. Proc Natl Acad Sci U S A **103:**12885–12890. http://dx.doi.org/10.1073/pnas.0603144103.
34. **Gallagher TM, Buchmeier MJ.** 2001. Coronavirus spike proteins in viral entry and pathogenesis. Virology **279:**371–374. http://dx.doi.org/10.1006/viro.2000.0757.
35. **Gallagher TM, Buchmeier MJ.** 1990. Monoclonal antibody-selected variants of MHV-4 contain substitutions and deletions in the E2 spike glycoprotein. Adv Exp Med Biol **276:**385–393. http://dx.doi.org/10.1007/978-1-4684-5823-7_53.
36. **Gallagher TM, Buchmeier MJ, Perlman S.** 1992. Cell receptor-independent infection by a neurotropic murine coronavirus. Virology **191:**517–522. http://dx.doi.org/10.1016/0042-6822(92)90223-C.
37. **Gallagher TM, Buchmeier MJ, Perlman S.** 1993. Dissemination of MHV4 (strain JHM) infection does not require specific coronavirus receptors. Adv Exp Med Biol **342:**279–284.
38. **Ontiveros E, Kim TS, Gallagher TM, Perlman S.** 2003. Enhanced virulence mediated by the murine coronavirus, mouse hepatitis virus strain JHM, is associated with a glycine at residue 310 of the spike glycoprotein. J Virol **77:**10260–10269. http://dx.doi.org/10.1128/JVI.77.19.10260-10269.2003.
39. **Miura TA, Travanty EA, Oko L, Bielefeldt-Ohmann H, Weiss SR, Beauchemin N, Holmes KV.** 2008. The spike glycoprotein of murine coronavirus MHV-JHM mediates receptor-independent infection and spread in the central nervous systems of Ceacam1a−/− Mice. J Virol **82:**755–763. http://dx.doi.org/10.1128/JVI.01851-07.
40. **McBride CE, Machamer CE.** 2010. A single tyrosine in the severe acute respiratory syndrome coronavirus membrane protein cytoplasmic tail is important for efficient interaction with spike protein. J Virol **84:**1891–1901. http://dx.doi.org/10.1128/JVI.02458-09.
41. **Kuo L, Masters PS.** 2002. Genetic evidence for a structural interaction between the carboxy termini of the membrane and nucleocapsid proteins of mouse hepatitis virus. J Virol **76:**4987–4999. http://dx.doi.org/10.1128/JVI.76.10.4987-4999.2002.
42. **Arndt AL, Larson BJ, Hogue BG.** 2010. A conserved domain in the coronavirus membrane protein tail is important for virus assembly. J Virol **84:**11418–11428. http://dx.doi.org/10.1128/JVI.01131-10.
43. **Narayanan K, Chen CJ, Maeda J, Makino S.** 2003. Nucleocapsid-independent specific viral RNA packaging via viral envelope protein and viral RNA signal. J Virol **77:**2922–2927. http://dx.doi.org/10.1128/JVI.77.5.2922-2927.2003.
44. **Narayanan K, Makino S.** 2001. Cooperation of an RNA packaging signal and a viral envelope protein in coronavirus RNA packaging. J Virol **75:**9059–9067. http://dx.doi.org/10.1128/JVI.75.19.9059-9067.2001.
45. **Pacciarini F, Ghezzi S, Canducci F, Sims A, Sampaolo M, Ferioli E, Clementi M, Poli G, Conaldi PG, Baric R, Vicenzi E.** 2008. Persistent replication of severe acute respiratory syndrome coronavirus in human tubular kidney cells selects for adaptive mutations in the membrane protein. J Virol **82:**5137–5144. http://dx.doi.org/10.1128/JVI.00096-08.
46. **de Haan CA, de Wit M, Kuo L, Montalto-Morrison C, Haagmans BL, Weiss SR, Masters PS, Rottier PJ.** 2003. The glycosylation status of the murine hepatitis coronavirus M protein affects the interferogenic capacity of the virus in vitro and its ability to replicate in the liver but not the brain. Virology **312:**395–406. http://dx.doi.org/10.1016/S0042-6822(03)00235-6.
47. **Ivanov KA, Thiel V, Dobbe JC, van der Meer Y, Snijder EJ, Ziebuhr J.** 2004. Multiple enzymatic activities associated with severe acute respiratory syndrome coronavirus helicase. J Virol **78:**5619–5632. http://dx.doi.org/10.1128/JVI.78.11.5619-5632.2004.
48. **Roberts A, Deming D, Paddock CD, Cheng A, Yount B, Vogel L, Herman BD, Sheahan T, Heise M, Genrich GL, Zaki SR, Baric R, Subbarao K.** 2007. A mouse-adapted SARS-coronavirus causes disease and mortality in BALB/c mice. PLoS Pathog **3:**e5. http://dx.doi.org/10.1371/journal.ppat.0030005.
49. **Frieman M, Yount B, Agnihothram S, Page C, Donaldson E, Roberts A, Vogel L, Woodruff B, Scorpio D, Subbarao K, Baric RS.** 2012. Molecular determinants of severe acute respiratory syndrome coronavirus pathogenesis and virulence in young and aged mouse models of human disease. J Virol **86:**884–897. http://dx.doi.org/10.1128/JVI.05957-11.
50. **Almeida MS, Johnson MA, Herrmann T, Geralt M, Wuthrich K.** 2007. Novel beta-barrel fold in the nuclear magnetic resonance structure of the replicase nonstructural protein 1 from the severe acute respiratory syndrome coronavirus. J Virol **81:**3151–3161. http://dx.doi.org/10.1128/JVI.01939-06.
51. **Gustin KM, Guan BJ, Dziduszko A, Brian DA.** 2009. Bovine coronavirus nonstructural protein 1 (p28) is an RNA binding protein that binds terminal genomic cis-replication elements. J Virol **83:**6087–6097. http://dx.doi.org/10.1128/JVI.00160-09.
52. **Versteeg GA, Bredenbeek PJ, van den Worm SH, Spaan WJ.** 2007. Group 2 coronaviruses prevent immediate early interferon induction by protection of viral RNA from host cell recognition. Virology **361:**18–26. http://dx.doi.org/10.1016/j.virol.2007.01.020.
53. **Roth-Cross JK, Martinez-Sobrido L, Scott EP, Garcia-Sastre A, Weiss SR.** 2007. Inhibition of the alpha/beta interferon response by mouse hepatitis virus at multiple levels. J Virol **81:**7189–7199. http://dx.doi.org/10.1128/JVI.00013-07.
54. **Rose KM, Elliott R, Martinez-Sobrido L, Garcia-Sastre A, Weiss SR.**

2010. Murine coronavirus delays expression of a subset of interferon-stimulated genes J Virol **84:**5656–5669.

55. **Menachery VD, Eisfeld AJ, Schafer A, Josset L, Sims AC, Proll S, Fan S, Li C, Neumann G, Tilton SC, Chang J, Gralinski LE, Long C, Green R, Williams CM, Weiss J, Matzke MM, Webb-Robertson BJ, Schepmoes AA, Shukla AK, Metz TO, Smith RD, Waters KM, Katze MG, Kawaoka Y, Baric RS.** 2014. Pathogenic influenza viruses and coronaviruses utilize similar and contrasting approaches to control interferon-stimulated gene responses. mBio **5**(3):e01174-14. http://dx.doi.org/10.1128/mBio.01174-14.
56. **Lei L, Ying S, Baojun L, Yi Y, Xiang H, Wenli S, Zounan S, Deyin G, Qingyu Z, Jingmei L, Guohui C.** 2013. Attenuation of mouse hepatitis virus by deletion of the LLRKxGxKG region of Nsp1. PLoS One **8:**e61166. http://dx.doi.org/10.1371/journal.pone.0061166.
57. **Narayanan K, Huang C, Lokugamage K, Kamitani W, Ikegami T, Tseng CT, Makino S.** 2008. Severe acute respiratory syndrome coronavirus nsp1 suppresses host gene expression, including that of type I interferon, in infected cells. J Virol **82:**4471–4479. http://dx.doi.org/10.1128/JVI.02472-07.
58. **Tanaka T, Kamitani W, DeDiego ML, Enjuanes L, Matsuura Y.** 2012. Severe acute respiratory syndrome coronavirus nsp1 facilitates efficient propagation in cells through a specific translational shutoff of host mRNA. J Virol **86:**11128–11137. http://dx.doi.org/10.1128/JVI.01700-12.
59. **Huang C, Lokugamage KG, Rozovics JM, Narayanan K, Semler BL, Makino S.** 2011. SARS coronavirus nsp1 protein induces template-dependent endonucleolytic cleavage of mRNAs: viral mRNAs are resistant to nsp1-induced RNA cleavage. PLoS Pathog **7:**e1002433. http://dx.doi.org/10.1371/journal.ppat.1002433.
60. **Jauregui AR, Savalia D, Lowry VK, Farrell CM, Wathelet MG.** 2013. Identification of residues of SARS-CoV nsp1 that differentially affect inhibition of gene expression and antiviral signaling. PLoS One **8:**e62416. http://dx.doi.org/10.1371/journal.pone.0062416.